

Self-catalytic etching of silicon: from nanowires to regular mesopores

L. Boarino^{1,1}, M. Destro¹, S. Borini¹, N. Pugno², A. Chiodoni³, F. Bellotti¹, and G. Amato¹

¹ Electromagnetic Div., Istituto Nazionale Ricerca Metrologica, Strada delle Cacce 91, 10135 Turin, Italy

² DISTR – Dept. of Structural and Geotechnical Engineering, Politecnico di Torino, Corso Duca degli Abruzzi 24, 10148 Turin, Italy

³ Department of Physics, Politecnico di Torino, Corso Duca degli Abruzzi 24, 10148 Turin, Italy

Received 19 March 2008, revised 20 January 2009, accepted 21 January 2009

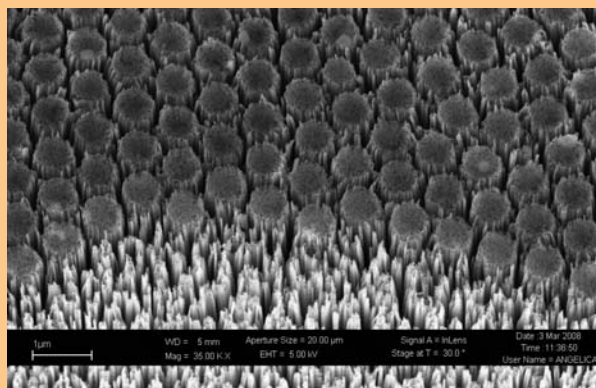
Published online 17 March 2009

PACS 62.23.Hj, 64.75.Yz, 81.16.Dn, 81.16.Hc, 81.16.Rf, 81.65.Cf

* Corresponding author: e-mail l.boarino@inrim.it

Metal assisted etching is a new promising technique for Silicon nanowires fabrication, but also for generating a new class of porous semiconductors with precise and controlled morphology, unavailable by electrochemical etching. The process and the morphology seem to be independent on substrate doping, but only on the crystallographic directions and metal patterning at the top surface. A preliminary investigation on some possible patterning techniques is reported, using porous silicon layers as pre-patterning tool, porous alumina and polystyrene nanospheres. The influence of the masking procedure on the final array of nanostructures is discussed.

Final morphology resulting from polystyrene nanosphere based patterning and metal assisted etching.



© 2009 WILEY-VCH Verlag GmbH & Co. KGaA, Weinheim

1 Introduction Metal assisted Silicon etching has been recently employed and investigated for nanowires fabrication [1–3]. The best aspect ratios and the most regular morphologies have been obtained by Ag deposition on Silicon substrates by precipitation of AgNO_3 solutions in HF or by thin films (<20 nm) thermal evaporation and HF dipping around room temperature (50 °C). The formation mechanism is ruled by local redox potential of the metal respect to silicon. This attracts the holes necessary to dissolution at the interface between the metal and the semiconductor. The metal clusters rapidly sink following the crystallographic directions, defining silicon walls or wires, depending on the metal particle distribution at surface [4, 5]. With layers of evaporated Ag of thickness under 20 nm or direct precipitation of Ag from AgNO_3 in HF, a wide range of silicon nanostructures can be obtained on a large surface, ranging from wires of 15 nm of diameter and tens

of micrometers in length to continuous pore walls or coalescence of multiple wires of different dimensions. Efforts have been addressed to form regular arrays of silicon nanowires, and in this work, to the achievement of ordered mesopores. The most successful method is represented at the moment by monodispersed silica nanospheres layers, tailored by RIE etching to reach the desired sphere diameter, then Ag thermal evaporation and HF etching [6]. Nanolithography has not been applied until now, probably due to the higher cost and to the reduced writable area. Aim of this work was the exploration of the use of polystyrene nanospheres as self-assembling mask layer to propagate an ordered pattern to silicon, and studying how this pre-patterning could affect the resulting metal assisted etching morphology. Playing with these methods, new applications in the fields of nanomechanics, electronics and bio-photonics could be explored [7–13].

2 Experimental

2.1 Patterning by porous silicon top-layer Different types of pre-patterning have been applied to n^+ - and p^+ -type silicon wafers (100 oriented, 10–20 m Ω cm, from MEMC Corp.). After standard cleaning procedures (RCA), the samples have been processed as follows: group A: direct Ag deposition by adding 0.02 mol/l of AgNO₃ in 5.0 mol/l HF solution in teflon cell at 60 °C. Group B: top layer formation, removal of PS top layer in KOH, meso-PS layer formation, Ag precipitation, final etching in HF. Group C: porous silicon formation limited to top layer [14] 20 mA, 10 s and successive Ag precipitation from AgNO₃, Ag removal by lift-off using the top layer as a sacrificial material, and etching as for group A. D: porous alumina masking layer, precipitation of Ag and self-catalytic etching. The etching duration was 10 minutes for all the groups of samples. In Fig. 1 the different processes are schematized for the first three groups.

2.2 Polystyrene nanospheres lithography For other groups of samples, polystyrene nanospheres (PSNS, from Estapore) lithography has been applied, following the most used literature recipes [15–17] for substrate hydrophilisation (RCA 1 hour 70 °C, H₂O:NH₄OH:H₂O₂ 5:1:1 70 °C or immersion in dodecyl sodium sulfonate 4% 24 h) then spinning with a low speed step at 400 rpm for PSNS dispersion and a successive step of 30 s at 1400 rpm for multiple layers removal. Since we used monodispersed nanospheres of 800 nm, an immediate optical inspection has been possible. Figure 2 gives an idea of the hydrophilicity of the substrate surface: white areas are related to the residual substrate hydrophobicity where no nanospheres could assembly, different grey-levels are single and multiple layers of nanospheres.

A few sets of samples have been exposed to RIE etching in O₂ atmosphere for times ranging from 10 minutes to 30 minutes, 100 W.

The sample have been then covered by 25 nm of thermally evaporated Ag. The Ag layer and the NSPS were

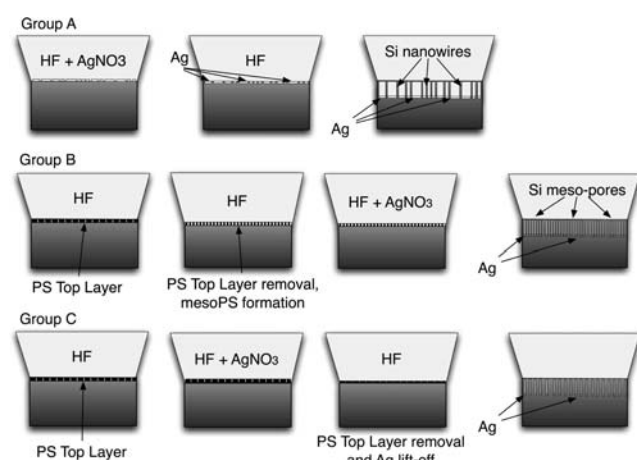


Figure 1 Scheme of the different processes for the first three groups of samples.

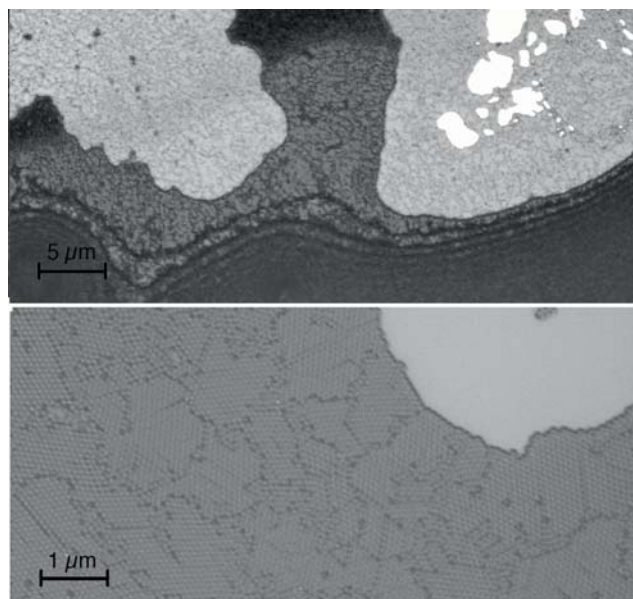


Figure 2 Optical inspection of the PSNS coverage: in white the hydrophobic silicon areas where no nanospheres could assembly, grey-levels are single and multiple layers of nanospheres (top, 20X). In the bottom part of the picture (100X) the self-ordered domains of a monolayer and a hydrophobic area.

removed by lift-off in few seconds of low power ultrasonic bath, and eventually etched for few minutes in a solution of HF:H₂O:H₂O₂ 1:4:1 starting by HF 50% (Fig. 3).

3 SEM analysis

3.1 Porous silicon patterning SEM analysis has been performed by a Zeiss Supra 40 FEG microscope. The former idea to study the morphology dependence of the metal assisted etching from the initial surface patterning has been carried out by using the top layer of porous silicon formed by highly doped substrates.

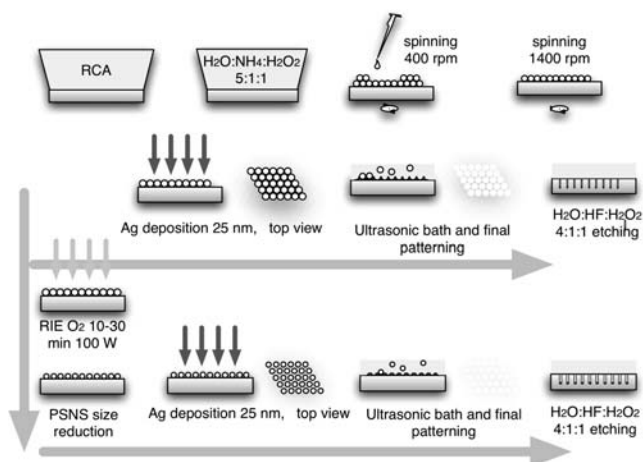


Figure 3 Scheme of the different processes for the PSNS patterning. After spinning one group of samples where deposited and another RIE processed for PSNS size reduction.

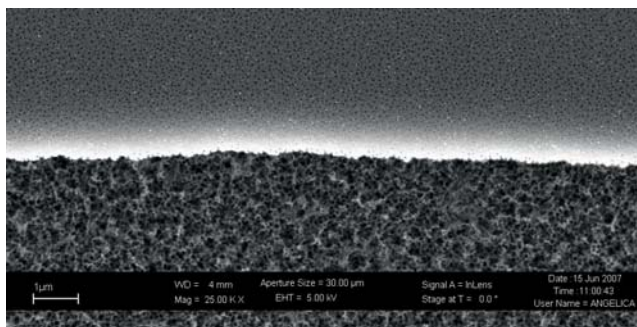


Figure 4 SEM top-view micrograph of a n^+ porous silicon sample in delaminated area. The difference between H-contaminated top-layer and underlying mesopores is clearly visible.

The presence of a top layer (about 200 nm thick) of different pore morphology respect to the mesostructures forming underneath is well known for highly doped wafers both of p- and n-type [14].

The formation of this layer is attributed to hydrogen contamination during chemo-mechanical-polishing.

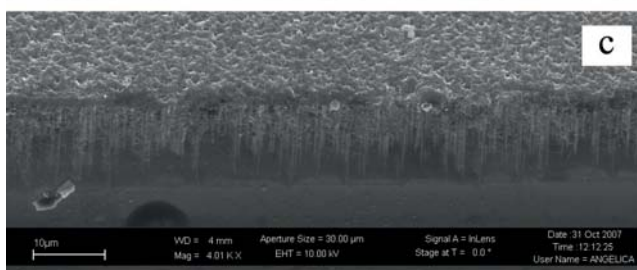
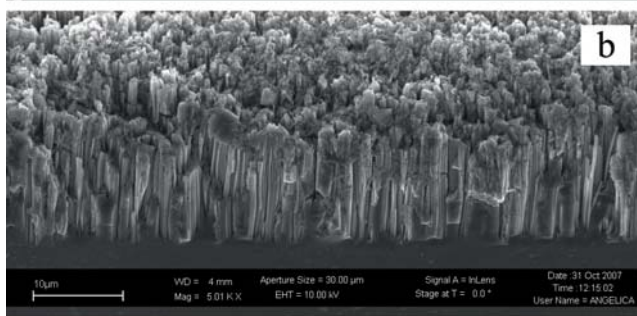
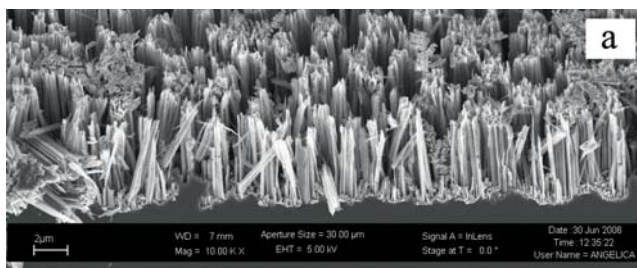


Figure 5 Three different morphologies of silicon metal-assisted etching resulting from different silver pre-patterning: a) silicon nanowires obtained by complete coverage of $AgNO_3$ precipitation in HF, b) structure obtained by precipitation in mesopores, c) low porosity obtained by precipitation on PS top-layer and removal before final etching.

In Fig. 4 a top view SEM microphotograph is shown for an n^+ -type porous silicon in proximity of a top-layer delamination due to cleavage. The different morphology is clearly visible. Almost independently by the applied current density, the pores of this H-contaminated layer are rather small, smaller than 20 nm, and the resulting porosity is around 50%.

We used this top layer as an irregular pre-indentation masking (and sacrificial) layer to obtain a low porosity material. Removing the top layer, forming a thin mesoporous layer and precipitating the Ag on this structure, a higher porosity layer is obtained.

SEM analysis shows a clear dependence of the porosity of the layers from the initial Ag patterning. With a complete coverage of precipitated Ag, a forest of nanowires is always obtained (Fig. 5a, group A).

The resulting structure is a coalescence of nanowalls and stuck nanowires ranging from 15 to 100 nanometers of diameter. With the deposition of Ag into the initiating mesopores, after top layer removal, a less dense nanostructure is obtained, more resembling a porous material rather than a disordered array of nanowires (Fig. 5b, group B), and with the pre-patterning through top-layer nanopores and successive lift-off of the Ag precipitated onto the whole area of the sample, a very low porosity is obtained, with small pores formed just in correspondence of few top layer nanopores (Fig. 5c, group B). For the group D the analysis is more complex, since the porous alumina layer is not HF resistant, and the material collapses and coalesces onto the silicon.

3.2 Polystyrene nanospheres patterning The SEM analysis of monolayers and multilayers of polystyrene nanospheres reveals that the product is not so mono-dispersed, and many defects of the self-assembled monolayers are related to smaller beads (400 nm) as visible in Fig. 6 (top). The other defects in the pre-patterning layers are mainly due to not hydrophobic areas. A more detailed study and investigation on this topic will guarantee higher coverage and a minor density of defects, but in any case many large domains of the order of hundreds of micrometers squared are obtainable with the current dispersion procedure.

In the following steps, the Ag deposition by thermal evaporation and nanobeads removal by few seconds in ultrasonic bath, a clear and undesired aggregation of metal clusters is evident (coverage of nanospheres in the bottom part of Fig. 6 and in the resulting Ag pattern), nevertheless an ordered structure of silver triangles is still present and aggregation does not affect the definition of the mesostructures resulting from the successive self catalytic etching.

Similar results have been obtained after Reactive Ion Etching in O_2 atmosphere, 100 W for 20 minutes. The PS nanospheres appear reduced in size (about 660 nm) and the corresponding Ag pattern after evaporation and beads removal clearly exhibits a circular corona of silver aggregates.

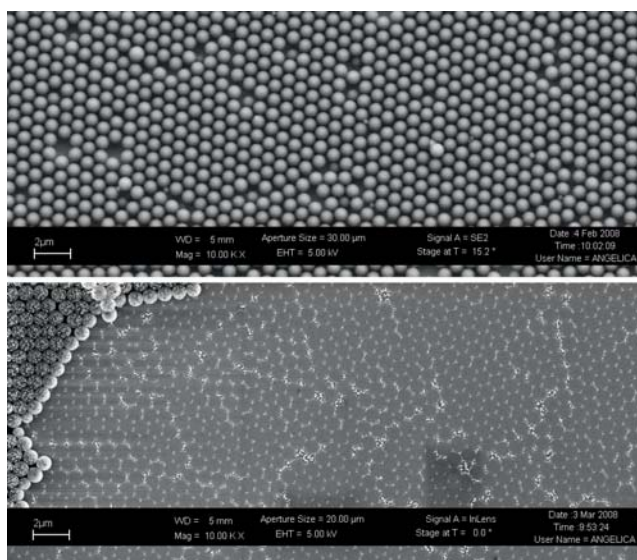


Figure 6 In the upper part of the picture, SEM micrograph of PSNS monolayer with some point defects due to a not complete monodispersion of nanobeads solution. In the bottom part, the metal patterns after Ag evaporation and PSNS removal.

Figure 7 shows the two patterns, without (top part of image) and after RIE treatment (bottom).

In Fig. 8, a complete range of structures resulting from the catalytic etching of this group of samples is shown. Where the Ag coverage is complete, due to the presence of

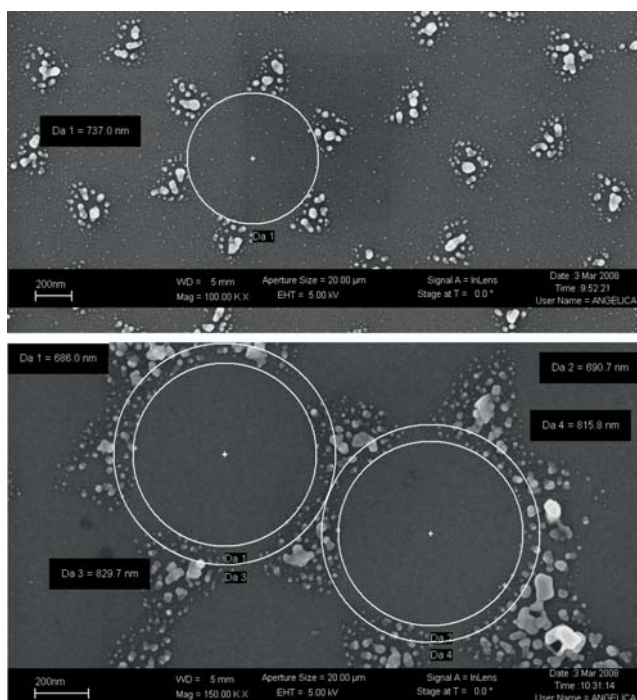


Figure 7 Final Ag patterns after PSNS removal in ultrasonic bath. Top: silver pattern of 800 nm PSNS monolayer. Bottom, the silver pattern after RIE processing for beads size reduction (660 nm) and Ag evaporation.

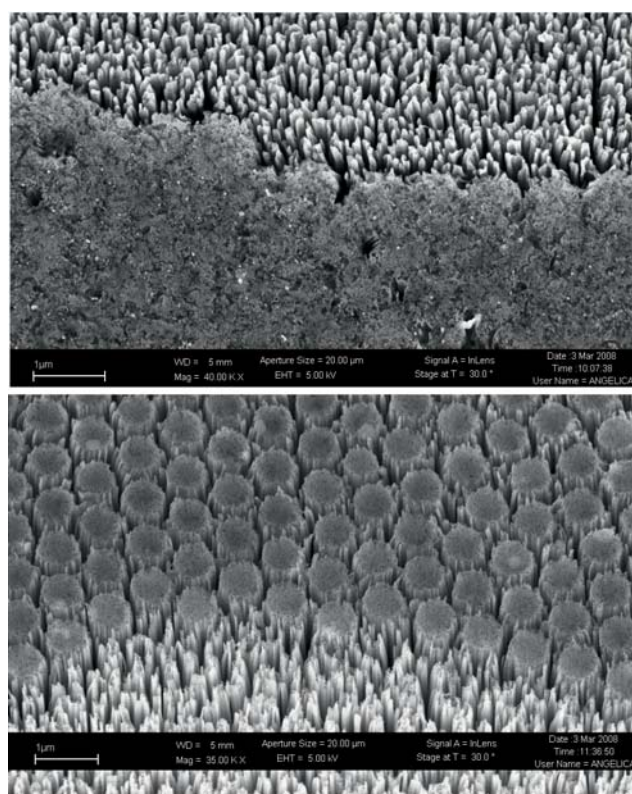


Figure 8 Final meso and nanostructures after metal-assisted etching of the pre-patterned samples. Top image, SEM micrograph of the propagated structure in vicinity of a hydrophobic area exhibiting a full coverage of nanowires. Bottom, a similar area of a RIE treated sample. The degeneration of the ordered mesopores towards continuous trenches is observable.

hydrophobic areas, a forest of silicon nanowires appears, while in the patterned areas by means of PSNS and Ag, a well defined and ordered structure of hexagons is propagated to silicon. In reality, this propagation is mainly due to the ordered metal patterns forming a regular array of pores during etching. The pattern obtained by RIE treatment of PSNS emphasize this pore structure, reaching in some areas almost the aspect of a trench.

After this preliminary study, smaller size beads can be used for nanopatterning, 450 nm down to 100 nm. The application of RIE allows good nanospheres size control with continuity from one monodispersion to the other. The achievement of an optimal patterning control could reasonably improve the realisation of nanowires and mesopores for a wide range of applications and fundamental studies.

4 Conclusions Mesoporous Silicon top layer and polystyrene nanospheres have been used to obtain different type of Ag pre-patterning for metal assisted etching. The preliminary use of PS top layer indicates the dependence of the resulting porous structure from the silver coverage, while the accurate control of dimensions typical of self-assembling nanospheres gives origin to an ordered array of

mesopores. RIE in O₂ has been successfully applied for PSNS size reduction.

References

- [1] X. Li and P. W. Bohn, *Appl. Phys. Lett.* **77**(16), 2572–2574 (2000).
- [2] K. Q. Peng, J. J. Hu, Y. J. Yan, Y. Wu, H. Fang, Y. Xu, S. T. Lee, and J. Zhu, *Adv. Funct. Mater.* **13**(2), 127–132 (2003).
- [3] T. Qiu, X. L. Wu, Y. F. Mei, G. J. Wan, P. K. Chu, and G. G. Siu, *J. Cryst. Growth* **277**(1–4), 143–148 (2005).
- [4] K. Q. Peng, J. J. Hu, Y. J. Yan, Y. Wu, H. Fang, Y. Xu, S. T. Lee, and J. Zhu, *Adv. Funct. Mater.* **16**(3), 387–394 (2006).
- [5] T. Qiu, X. L. Wu, G. G. Siu, and P. K. Chu, *J. Electron. Mater.* **35**(10), 1879–1884 (2006).
- [6] Z. P. Huang, H. Fang, and J. Zhu, *Adv. Mater.* **19**(5), 744 (2007).
- [7] L. Pescini, A. Tilke, R. H. Blick, H. Lorenz, J. P. Kotthaus, W. Eberhardt, and D. Kern, *Nanotechnology* **10**(4), 418–420 (1999).
- [8] M. Menon, D. Srivastava, I. Ponomareva, and L. A. Chernozatonskii, *Phys. Rev. B* **70**(12), 125313 (2004).
- [9] N. Verplanck, E. Galopin, J. C. Camart, V. Thomy, Y. Coffinier, and R. Boukherrou, *Nano Lett.* **7**(3), 813–817 (2007).
- [10] K. Q. Peng, Y. Xu et al., *Small* **1**(11), 1062–1067 (2005).
- [11] B. M. Kayes, M. A. Filler, M. C. Putnam, M. D. Kelzenberg, N. S. Lewis, and H. A. Atwater, *Appl. Phys. Lett.* **91**(10), 103110 (2007).
- [12] A. A. Talin, L. L. Hunter, F. Leonard, and B. Rokad, *Appl. Phys. Lett.* **89**(15), 153102 (2006).
- [13] X. T. Zhou, J. Q. Hu, C. P. Li, D. D. Ma, C. S. Lee, and S. T. Lee, *Chem. Phys. Lett.* **369**(1–2), 220–224 (2003).
- [14] V. Chamard, G. Dolino, and F. Muller, *J. Appl. Phys.* **84**(12), 6659–6666 (1998).
- [15] J. C. Hulteen and R. P. Van Duyne, *J. Vac. Sci. Technol. A* **13**(3), 1553 (1995).
- [16] B. G. Prevo, D. M. Kuncicky, and O. D. Velez, *Colloid Surf. A* **311**(1–3), 2–10 (2007).
- [17] J. Rybczynski, U. Ebels, and M. Giersig, *Colloids Surf. A* **219**(1–3), 1–6 (2003).